EVS30 Symposium
Stuttgart, Germany, October 9 - 11, 2016

Advanced Torque Vectoring for Yaw Stability Enhancement of a Four Wheel Drive Electric Vehicle

Chansu Jung[1], Jinho Kim[1], Kanghyun Nam[2]
[1]*School of Mechanical Engineering, Yeungnam University, address,email*
[2]*(corresponding author) School of Mechanical Engineering, Yeungnam University, khnam@yu.ac.kr*

Abstract

This paper presents a method for driving torque vectoring control of four wheel drive electric vehicles with in-wheel-motors and an active front steering motor. In general, since a electric vehicle equipped with in-wheel-motors have high dynamic responses over internal combustion engine vehicles, it is expected that high speed and precise dynamic motion control such as traction or yaw motion control, etc.. In this paper, we designed the yaw motion control based on a proposed torque vectoring method for improving cornering performances. In order to realize precise cornering force generation, we designed two types of lateral tire force controllers and have done comparative study on control performances of each control method. Computer simulations using commercial software CarSim have been performed to verify the effectiveness of a proposed controller. Based on robust controller design for yaw moment control and lateral tire force control, the vehicle cornering stability and handling performances can be provided at the same time.

Keywords: Electric vehicle, Torque vectoring, Yaw stability. CarSim simulation.

1 Introduction

As concerns over air pollution and global warming continue to mount, the electric vehicle market is predicted to expand at a significantly rapid rate. Increasing fuel costs, government purchase incentives, increasing fuel economy standards, and increased vehicle availability will benefit several types of electric vehicles (e.g., hybrid electric vehicles, battery electric vehicle, etc.) to varying degrees. In reality, electric vehicles are considered as a promising technology for drastically reducing the environmental burden of road transport. More than a decade ago and also more recently, they were advocated by many governments and automotive manufacturers as an important element in reducing CO_2 emissions of particularly passenger cars and light commercial vehicles as well as emissions of pollutants and noise. Over the recent years, almost all of automotive manufacturers in the worlds have released electric vehicles, for even great reductions in CO_2 emissions that contribute to global climate change. Compared with internal combustion engine vehicles, electric vehicles with in-wheel motors have several advantages in the viewpoint of motion control [1]–[3],

1. The torque generation of driving motors is very fast and accurate.
2. The driving torque can be easily measured and it can be used in estimating the road conditions.
3. Each wheel with an direct drive motor can be independently controlled.

In general, the purpose of vehicle motion controls is to prevent unintended vehicle behavior through active vehicle control and assist drivers in maintaining controllability and stability of vehicles [4], [5]. In this paper, a new control scheme, utilizing active front steering and independent in-wheel motor control, is presented as a practical solution to the vehicle cornering stability issues in a four wheel drive electric vehicle. A two-degree-of-freedom(2-DOF) control method, which is widely applied in many motion control systems, is used to generate control yaw moment to be controlled for stabilizing vehicle motion.

2 Vehicle and Tire Models for Vehicle Motion

2.1 Lateral Vehicle Dynamics

In this section, a three degree-of-freedom (3–DOF) yaw plane model is introduced to describe the lateral motion of electric vehicles. The yaw plane representation with independent motor torque control is shown in Fig. 1 [9].

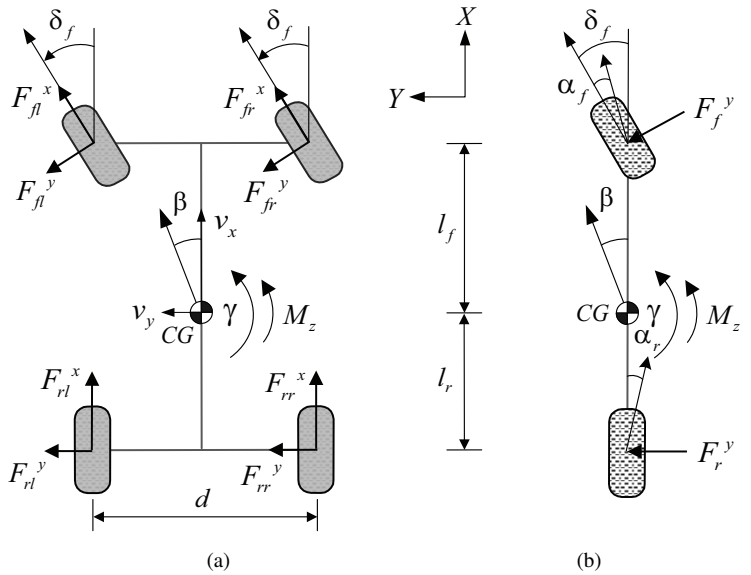

Figure 1: Planar vehicle model: (a) Four wheel model, (b) Single track model (i.e., bicycle model).

The governing equations for longitudinal and lateral motions are given by

$$ma_y = \sum_{i=1}^{2}(F_i^x \sin\delta_f + F_i^y \cos\delta_f) + \sum_{i=3}^{4}(F_i^y) \tag{1}$$

where the steering angles of front left and right wheels are assumed to be the same (i.e., = δ_f). The yaw moment balance equation with respect to point CG is

$$I_z\dot{\gamma} = \sum_{i=1}^{2} l_f(F_i^x \sin\delta_f + F_i^y \cos\delta_f) - \sum_{i=3}^{4} l_r(F_i^y) + M_z \tag{2}$$

where the yaw moment, M_z, indicates a direct yaw moment control input, which is generated by the independent torque control of in-wheel motors and is used to stabilize the vehicle motion, and can be calculated as follows:

$$M_z \;=\; \frac{d}{2}(F_{rr}^x - F_{rl}^x) + \frac{d}{2}(F_{fr}^x - F_{fl}^x)\cos\delta_f \tag{3}$$

Here, longitudinal tire forces can be obtained from a driving force observer which is designed based on wheel dynamics [6].

For small tire slip angles, the lateral tire forces can be linearly approximated as follows:

$$\bar{F}_f^y = -2C_f\alpha_f = -2C_f\left(\beta + \frac{\gamma l_f}{v_x} - \delta_f\right) \quad (4)$$

$$\bar{F}_r^y = -2C_r\alpha_r = -2C_r\left(\beta - \frac{\gamma l_r}{v_x}\right) \quad (5)$$

2.2 Lateral Tire Force Model

The tires, which generate longitudinal, lateral forces and moments, have a significant effect on the dynamic characteristics of vehicles. These tire forces are explained by complex relation between tire-road friction, normal force on the tire, variable slip angles, and elastic tire properties. In order to model the tire force generation, several tire models have been developed. A widely used empirical tire model (i.e., magic formula tire model) is dominantly based on empirical formulations deriving from tire test data and a large number of tire parameters. Hence, it is not suitable for real-time application to vehicle control systems. To avoid complex calculation and using tire test data, In this paper, we use linearized tire force model . In order to account for transient behavior of tires, a typical dynamic model, which is the first order dynamics, is used and expressed as follows [9]:

$$\tau_{lag,i}\dot{F}_i^y + F_i^y = \bar{F}_i{}^y \quad (6)$$

where $\tau_{lag,i}$ is the relaxation time constant and calculated from the longitudinal vehicle velocity and tire relaxation length, which is the approximate distance needed to build up tire forces, and $\bar{F}_i{}^y$ is the lateral tire force from a linear tire model. From (4) and (5), the dynamic lateral tire force models for front and rear tires are obtained as follows:

$$\dot{F}_f^y = -\frac{1}{\tau_{lag,f}}F_f^y - \frac{2C_f}{\tau_{lag,f}}\beta - \frac{2l_fC_f}{\tau_{lag,f}v_x}\gamma + \frac{2C_f}{\tau_{lag,f}}\delta_f \quad (7)$$

$$\dot{F}_r^y = -\frac{1}{\tau_{lag,r}}F_r^y - \frac{2C_r}{\tau_{lag,r}}\beta + \frac{2l_rC_r}{\tau_{lag,r}v_x}\gamma \quad (8)$$

where $\tau_{lag,f}$ and $\tau_{lag,r}$ are the relaxation time constants for front and rear tires, respectively.

3 Design of a Yaw Stability Controller

3.1 Overall Structure of Proposed Control System

The main control objective of proposed control system is to improve safety and stability in all driving regions and in the presence of undesirable external conditions such as strong wind or changing tire-road conditions. The overall control scheme in Fig. 2 is as follows.

1. First, the desired vehicle responses are obtained from a linear vehicle model and driver's commands such as a steering angle and vehicle speed.
2. Second, the yaw stability controller is designed to make vehicle yaw rate follow reference yaw rate. The novel yaw moment observer (YMO), which was proposed by Fujimoto. et. al. [7], is used for rejecting yaw moment disturbances caused by lateral wind, unbalanced road conditions, and unbalanced tire pressure.
3. Third, the robust lateral tire force controller is designed to stabilize the lateral vehicle motion by controlling the front steering angle. In this paper, a lateral tire force control method, was proposed in [8], is used for realizing the proposed control method.
4. Finally, the control allocation based on optimal linear programming is carried out for deciding optimal control commands to controllable actuators, e.g., four in-wheel motors and the front power steering motor.

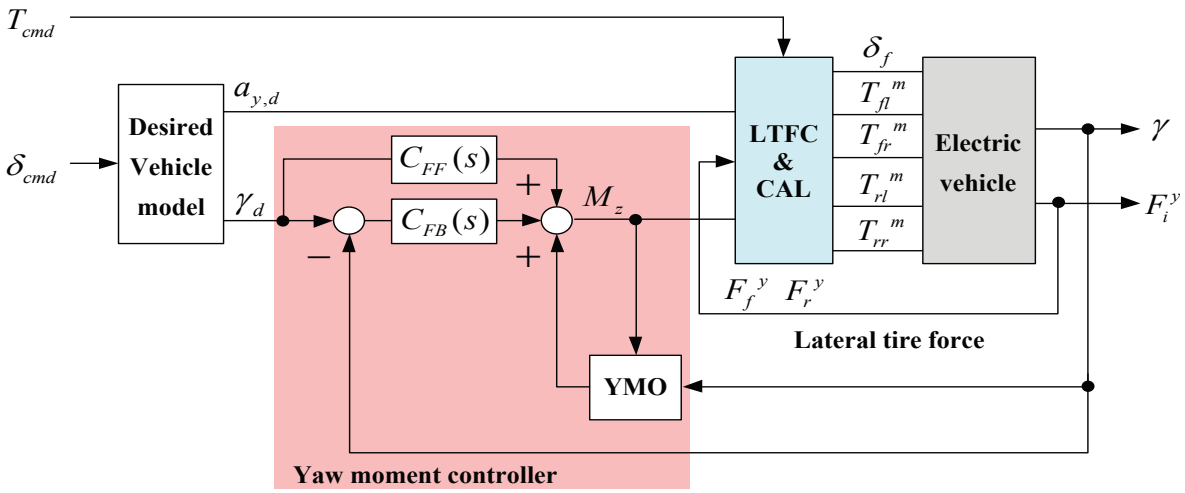

Figure 2: Block diagram of the overall cornering stability control system.

3.2 Design of Desired Vehicle Model

The objective of the stability control is to improve the vehicle steadiness and transient response properties, enhancing vehicle handling performance and maintaining stability in those cornering maneuvers, i.e., the yaw rate γ or side slip angle β of the vehicle should be close to desired vehicle responses (γ_d and β_d). Desired vehicle responses are defined based on driver's cornering intention (e.g., drivers' steering command and vehicle speed). Desired vehicle lateral acceleration and yaw rate for given steering angle and vehicle speed are obtained as follows [9]:

$$a_{y,d} = v_x(\gamma_d + s\beta_d) \tag{9}$$

$$\gamma^* = \left(\frac{\omega_\lambda}{s+\omega_\lambda}\right) \cdot \frac{1}{1+K_s v_x^2} \frac{v_x}{l} \cdot \delta_f \tag{10}$$

$$K_s = \frac{m(l_r C_r - l_f C_f)}{2l^2 C_f C_r} \tag{11}$$

where ω_λ and ω_β are cutoff frequencies (e.g., in this paper, ω=15 rad/s is chosen) of desired model filters, respectively, K_s is the vehicle stability factor, which explains the steering characteristics of the vehicles. The sign of $l_r C_r - l_f C_f$ in K_s represents vehicle motion behavior by steering action that illustrated in Fig. 3.

3.3 Design of a Robust Lateral Tire Force Controller

For the comparison study, the feedforward lateral tire force control is also employed and is depicted as shown in Fig. 5. This control scheme can not provide the robustness against vehicle parameter changes and road condition changes. Thus, the precise lateral tire force control can not be achieved with this feedforward scheme only.
Dynamics lateral tire force model (7) is used for control design. The lateral tire force is generated by controlling steering angle and side slip angle β and yaw rate γ, which affect lateral tire force generation, are also generated by steering angle control. Therefore, we can obtain a dynamic lateral tire force model which is single-input and single-output (SISO) system as follows:

$$\dot{F}_f^y = -\frac{1}{\tau_{lag,f}} F_f^y - \frac{2C_f}{\tau_{lag,f}}\beta - \frac{2l_f C_f}{\tau_{lag,f} v_x}\gamma + \frac{2C_f}{\tau_{lag,f}}\delta_f \tag{12}$$

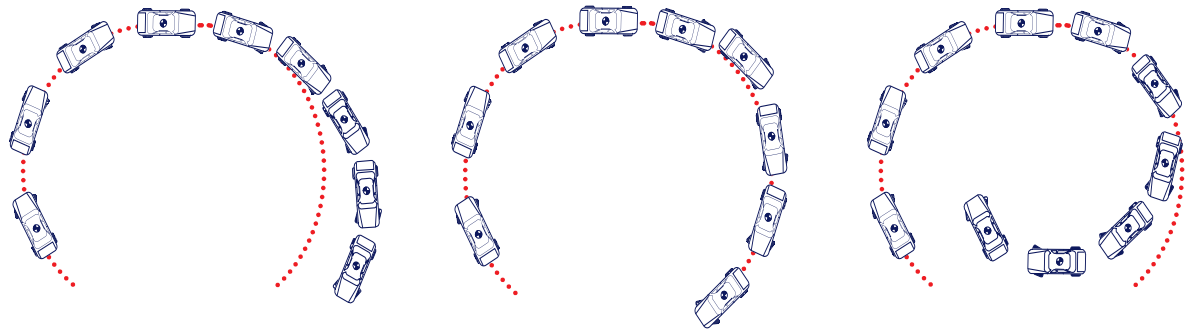

(a) (b) (c)

Figure 3: Three types of cornering behavior. (a) Under-steer cornering, (b) Neutral-steer cornering, (c) Over-steer cornering.

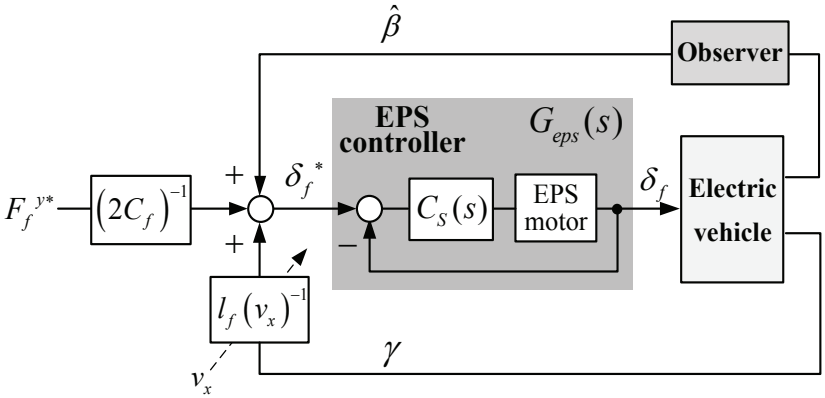

Figure 4: Block diagram of the feed-forward lateral tire force controller (i.e., without lateral tire force feedback).

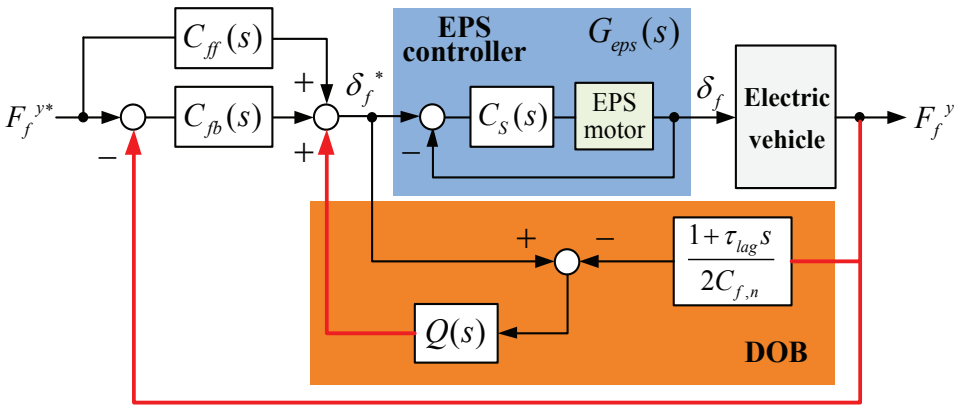

Figure 5: Block diagram of the robust lateral tire force controller (see [8])

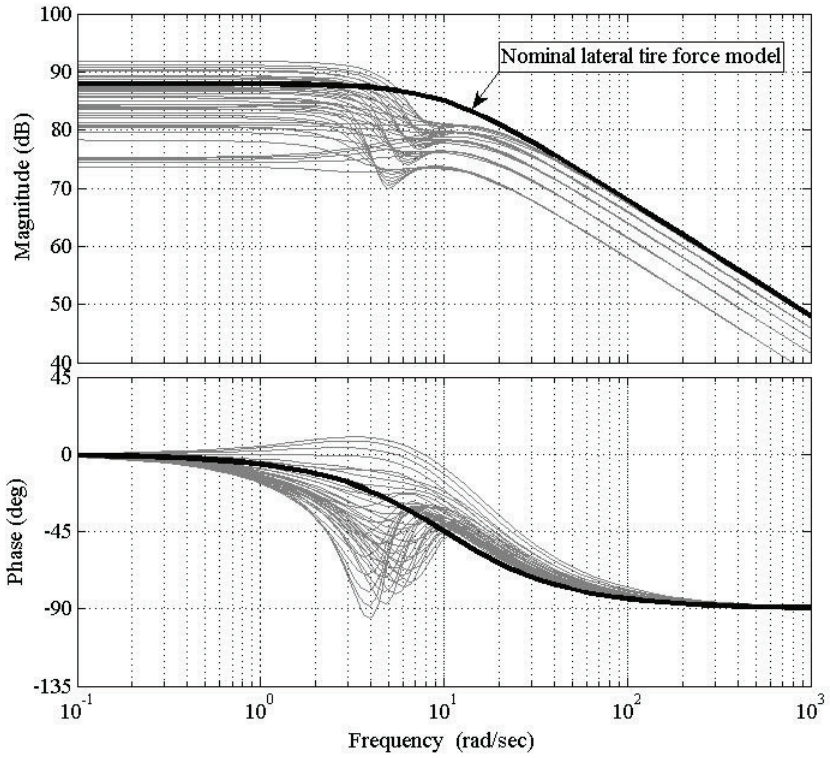

Figure 6: Frequency response of lateral tire force model.

$$F_f^y(s) = -\frac{2C_f}{1+\tau_{lag,f}s}\left(G_{\beta\delta_f}(s) + \frac{l_f}{v_x}G_{\gamma\delta_f}(s) - 1\right)\delta_f(s) \tag{13}$$

Nominal lateral tire force model is obtained from the dynamic lateral tire force model (9) and expressed as follows [8]:

$$\dot{F}_f^y = -\frac{1}{\tau_{lag,f}}F_f^y + \frac{2C_{fn}}{\tau_{lag,f}}\delta_f + F_d^y \tag{14}$$

where disturbance F_d^y indicates lumped lateral force disturbance and expressed as

$$F_d^y = -\frac{2C_f}{\tau_{lag,f}}\left(\beta + \frac{l_f\gamma}{v_x} - d\right) \tag{15}$$

From (14), a transfer function for the nominal lateral tire force model is obtained [8]

$$P_n(s) = \frac{F_f^y(s)}{\delta_f(s)} = \frac{2C_{fn}}{1+\tau_{lag,f}s} \tag{16}$$

where C_{fn} is the front tire cornering stiffness for a value on a high–μ road (i.e., μ=1.0).
The thick continuous line in Fig. 6 represents the nominal model $P_n(s)$. Considering driving conditions of usual vehicles (e.g., Almost all of the vehicles drive on dry asphalt.), the nominal model was chosen as shown in (16).

4 Driving Torque Vectoring

In this section, a control allocation method is presented. Since an electric vehicle to be controlled has three control inputs and five controllable outputs, which are four in-wheel motors and front EPS motor, we should consider actuator redundancy issue for ensuring efficient control allocation. The five control variables have to satisfy the following equality constraints given by force and moment balance equations.

- The sum of the generated longitudinal tire forces on the four wheels should be equal to the required total longitudinal force to meet driver's driving command.

$$F_{cmd} = F_f^y \sin\delta_f + F_{fl}^x \cos\delta_f + F_{fr}^x \cos\delta_f + F_{rl}^x + F_{rr}^x \tag{17}$$

- The sum of the generated lateral tire forces on the four wheels should be equal to the required total lateral force to follow the desired lateral force.

$$ma_y = F_f^y \cos\delta_f + F_r^y + F_{fl}^x \sin\delta_f + F_{fr}^x \sin\delta_f \tag{18}$$

- The sum of the generated yaw moment by longitudinal and lateral tire forces should be equal to the required total yaw moment to follow the desired yaw rate response.

$$\begin{aligned} M_z = l_f F_f^y \cos\delta_f - l_r F_r^y + F_{fl}^x (l_f \sin\delta_f - \tfrac{d}{2}\cos\delta_f) \\ + F_{fr}^x (l_f \sin\delta_f + \tfrac{d}{2}\cos\delta_f) - \tfrac{d}{2} F_{rl}^x + \tfrac{d}{2} F_{rr}^x \end{aligned} \tag{19}$$

where F_{cmd} is driver's driving force command calculated from an acceleration pedal sensor and lateral tire forces are directly measured.

4.1 Friction Circle

The friction circle concept is used in the optimal control allocation problem as a part of the cost function, which attempts to maximize the tire forces [9].
Note that the friction limit for a tire, regardless of direction, is determined by the coefficient of friction times the vertical tire force. Thus, it is clear that the friction can be used for longitudinal tire force, lateral tire force, or a combination of the two forces. The longitudinal, lateral, and vertical tire forces acting on the tires have the following relationship:

$$F_i^{x2} \; + \; F_i^{y2} \; = \; (\mu F_i^z)^2 \tag{20}$$

where μ is the friction coefficient, the vertical tire force F_i^z is obtained from following equations in which the effects of weight transfer due to lateral and longitudinal accelerations are considered.

$$\begin{aligned} F_i^z \; &= \; mg \left[\frac{l_r}{2l} - \frac{a_x}{g}\frac{h_{CG}}{2l} \mp \frac{a_y}{g}\frac{l_r h_{CG}}{dl} \right], \;\; i = 1, 2 \\ F_i^z \; &= \; mg \left[\frac{l_f}{2l} + \frac{a_x}{g}\frac{h_{CG}}{2l} \mp \frac{a_y}{g}\frac{l_f h_{CG}}{dl} \right], \;\; i = 3, 4. \end{aligned} \tag{21}$$

4.2 Torque Vectoring Algorithm

Based on equality constraints (17)–(19) and the concept of the friction circle, a optimization problem is formulated by defining the cost function as follows:

$$\begin{aligned} &\text{minimize} \quad J \\ &\text{subject to} \quad Ax = y \end{aligned} \tag{22}$$

where J is defined as

$$J \; = \; \frac{1}{2}\sum_{i=1}^{4} (\mu_i)^2 \; = \; \frac{1}{2}\sum_{i=1}^{4} \left(\frac{F_i^{x2} + F_i^{y2}}{F_i^{z2}} \right)$$

$$x = \left[\; F_f^y, \; F_{fl}^x, \; F_{fr}^x, \; F_{rl}^x, \; F_{rr}^x \; \right]^T,$$

$$y = \begin{bmatrix} F_{cmd} \\ ma_{y,d} - F_r^y \\ M_z + l_r F_r^y \end{bmatrix},$$

$$A = \begin{bmatrix} \sin\delta_f & \cos\delta_f & \cos\delta_f & 1 & 1 \\ \cos\delta_f & \sin\delta_f & \sin\delta_f & 0 & 0 \\ l_f\cos\delta_f & l_f\sin\delta_f - \frac{d}{2}\cos\delta_f & l_f\sin\delta_f + \frac{d}{2}\cos\delta_f & -\frac{d}{2} & \frac{d}{2} \end{bmatrix}$$

and A, x, and y in (22) are expressed as above.
The defined cost function J in (22) can be expressed as a quadratic form as follows:

$$J \; = \; \frac{1}{2} x^T Q x \tag{23}$$

where

$$Q = \begin{bmatrix} \frac{2}{(F_f^z)^2} + \frac{2(\frac{l_f}{l_r})^2}{(F_r^z)^2} & 0 & 0 & 0 & 0 \\ 0 & \frac{1}{(F_{fl}^z)^2} & 0 & 0 & 0 \\ 0 & 0 & \frac{1}{(F_{fr}^z)^2} & 0 & 0 \\ 0 & 0 & 0 & \frac{1}{(F_{rl}^z)^2} & 0 \\ 0 & 0 & 0 & 0 & \frac{1}{(F_{rr}^z)^2} \end{bmatrix}$$

A weighting matrix Q is derived from a pre-defined cost function and vehicle dynamics equations.
The cost function J in (22) is

$$\begin{aligned} J &= \frac{1}{2}\sum_{i=1}^{4}\left(\frac{F_i^{x\,2} + F_i^{y\,2}}{F_i^{z\,2}}\right) \\ &= \frac{1}{2}\left(\frac{F_{fl}^{y\,2}}{F_{fl}^{z\,2}} + \frac{F_{fr}^{y\,2}}{F_{fr}^{z\,2}}\right) + \frac{1}{2}\left(\frac{F_{rl}^{y\,2}}{F_{rl}^{z\,2}} + \frac{F_{rr}^{y\,2}}{F_{rr}^{z\,2}}\right) + \frac{1}{2}\left(\frac{F_{fl}^{x\,2}}{F_{fl}^{z\,2}} + \frac{F_{fr}^{x\,2}}{F_{fr}^{z\,2}} + \frac{F_{rl}^{x\,2}}{F_{rl}^{z\,2}} + \frac{F_{rr}^{x\,2}}{F_{rr}^{z\,2}}\right). \end{aligned} \tag{24}$$

Since the lateral tire forces vary with respect to weight transfer, we can assume following relationship between lateral tire forces acting on left and right tires by considering the ratio of vertical tire forces.

$$\begin{aligned} F_{fl}^y &= \frac{F_{fl}^z}{F_{fl}^z + F_{fr}^z} \cdot F_f^y \\ F_{fr}^y &= \frac{F_{fr}^z}{F_{fl}^z + F_{fr}^z} \cdot F_f^y \\ F_{rl}^y &= \frac{F_{rl}^z}{F_{rl}^z + F_{rr}^z} \cdot F_r^y \\ F_{rr}^y &= \frac{F_{rr}^z}{F_{rl}^z + F_{rr}^z} \cdot F_r^y \end{aligned} \tag{25}$$

where it is assumed that $F_f^y = F_{fl}^y + F_{fr}^y$, $F_r^y = F_{rl}^y + F_{rr}^y$, and $l_f F_f^y = l_r F_r^y$ (this is a kinematic relationship between front and rear lateral tire forces which do not make yaw moment).

From (25), the cost function (24) can be rewritten as follows,

$$
\begin{aligned}
J &= \frac{1}{2}\left(\frac{2F_f^{y2}}{(F_{fl}^z+F_{fr}^z)^2}+\frac{2F_r^{y2}}{(F_{rl}^z+F_{rr}^z)^2}\right)+\frac{1}{2}\left(\frac{F_{fl}^{x\,2}}{F_{fl}^{z\,2}}+\frac{F_{fr}^{x\,2}}{F_{fr}^{z\,2}}+\frac{F_{rl}^{x2}}{F_{rl}^{z\,2}}+\frac{F_{rr}^{x\,2}}{F_{rr}^{z\,2}}\right) \\
&= \frac{1}{2}\left(\frac{2}{(F_f^z)^2}+\frac{2(\frac{l_f}{l_r})^2}{(F_r^z)^2}\right)F_f^{y2}+\frac{1}{2}\left(\frac{F_{fl}^{x\,2}}{F_{fl}^{z\,2}}+\frac{F_{fr}^{x\,2}}{F_{fr}^{z\,2}}+\frac{F_{rl}^{x2}}{F_{rl}^{z\,2}}+\frac{F_{rr}^{x\,2}}{F_{rr}^{z\,2}}\right),
\end{aligned}
\tag{26}
$$

Using Lagrange's theorem, the unique solution to optimization problem (22) is obtained as follows,

$$
x^* = Q^{-1}A^T(AQ^{-1}A^T)^{-1}y. \tag{27}
$$

5 Simulation Results

Computer simulations were performed to evaluate the proposed stability control system. Based on specifications of an experimental four wheel drive electric vehicle, the simulation vehicle model was obtained using CarSim. Simulation environment using CarSim model and Matlab/simulink were constructed for implementation of proposed control algorithms. The proposed cornering stability control system based on an advanced torque vectoring was evaluated through co-simulation for step steering tests. Fig. 8 shows the results of computer simulation.

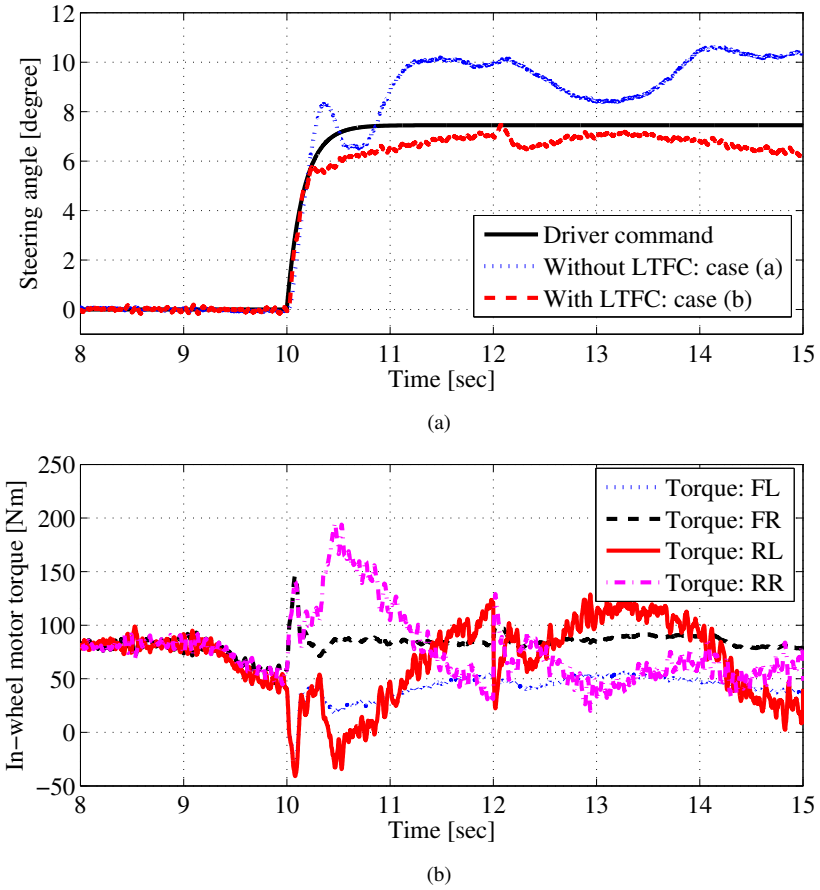

Figure 7: Simulation results for step steering at 60 km/h: (a) Steering angle, (b) In-wheel motor torque.

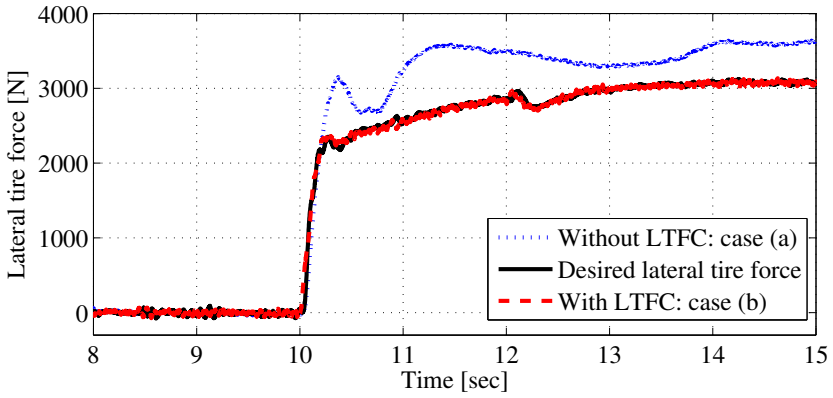

(a)

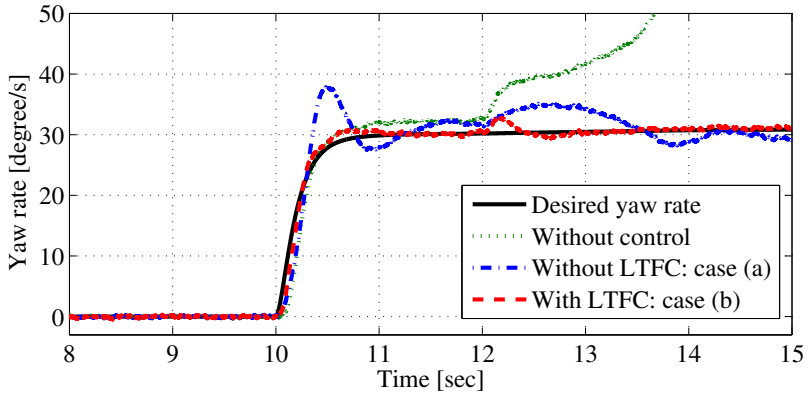

(b)

Figure 8: Simulation results for step steering at 60 km/h: (a) Lateral tire force, (b) Yaw rate.

Acknowledgments

This work is supported by Civil-Military Technology Cooperation Program 16-CM-EN-17.

References

[1] Y. Hori, "Future vehicle driven by electricity and control-research on four-wheel-motored "UOT Electric March II"," *IEEE Trans. Ind. Electron.*, vol. 51, no. 5, pp. 654–962, Oct. 2004.

[2] S. Sakai, H. Sado, and Y. Hori, "Motion control in an electric vehicle with four independently driven in-wheel motors," *IEEE/ASME Trans. Mechatron.*, vol. 4, no. 1, pp. 9–16, Mar. 1999.

[3] N. Mutoh and Y. Nakano, ''Dynamics of front-and-rear-wheel-independent-drive-type electric vehicles at the time of failure," *IEEE Trans. Ind. Electron.*, vol. 59, no. 3, pp. 1488–1499, Mar. 2012.

[4] K. Nam, Y. Kim, S. Oh, and Y. Hori, ''Steering angle-disturbance observer(SA-DOB) based yaw stability control for electric vehicles with in-wheel motors," in *Proc. of Int. Conf. on Control Automation and Systems (ICCAS),* , pp. 1303–1307, Dec. 2010.

[5] J. Ahmadi, A. K. Sedigh, and M. Kabganian, "Adaptive vehicle lateral-plane motion control using optimal tire friction forces with saturation limits consideration," *IEEE Trans. Veh. Technol.*, vol. 58, no. 8, pp. 4098–4107, Sep. 2009.

[6] H. Sado, S. Sakai, and Y. Hori, ''Road condition estimation for traction control in electric vehicle," in *Proc. IEEE Int. Symp. Ind. Electron.(ISIE 99)* , Jul. 1999, pp. 973–978.

[7] H. Fujimoto, A. Tsumasaka, and T. Noguchi, ‘‘Direct yaw-moment control of electric vehicle based on cornering stiffness estimation,” in *Proc. of IEEE IECON*, Nov. 2005.

[8] K. Nam, H. Fujimoto and Y. Hori, ”Advanced Motion Control of Electric Vehicles Based on Robust Lateral Tire Force Control via Active Front Steering,” *IEEE/ASME Trans. Mechatron.*, vol. 19, no. 1, pp. 289-299, Feb. 2014.

[9] R. Rajamani, $Vehicle\ Dynamics\ and\ Control$. New York: Springer-Verlag, 2005.

Authors

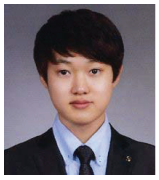

Chansu Jung received the B.S.degree in mechanical engineering from Yeungnam University, Gyeongbuk, Republic of Korea, in 2017, and is now a M.S degree student.

Jinho Kim received Ph.D. degree in Mechanical Engineering from University of California, Berkeley, USA, in 2005. Now he works as the Associate Professor at School of Mechanical Engineering, Yeungnam University, Korea. His research interests include electric machine, vibration, and design.

Kanghyun Nam received the B.S.degree in mechanical engineering from Kyungpook National University, Daegu, Republic of Korea, in 2007, the M.S.degree in mechanical engineering from Korea Advanced Institute of Science and Technology, Daejeon, Republic of Korea, in 2009, and the Ph.D.degree in electrical engineering from The University of Tokyo, Tokyo, Japan, 2012. From 2012 to 2015, he was a Senior Engineer with Samsung Electronics Co., Ltd., Gyeonggi-do, Republic of Korea. Since 2015, he has been an Assistant Professor with the School of Mechanical Engineering, Yeungnam University, Gyeongbuk, Republic of Korea.